

Low-temperature dynamics of confined methyl iodide

R. M. Dimeo* and D. A. Neumann

NIST Center for Neutron Research, National Institute of Standards and Technology, 100 Bureau Drive, STOP 8562, Gaithersburg, Maryland 20899

(Received 20 June 2000; published 11 December 2000)

The rotational tunneling and librational excitations of the one-dimensional quantum rotor, methyl iodide, confined in porous glass monoliths (mean pore diameter of 58 Å) have been investigated using incoherent inelastic neutron scattering. When the pores are completely filled with the solid at low temperatures ($5\text{ K} < T < 35\text{ K}$), the system exhibits a tunneling spectrum composed of two sets of inelastic peaks: one set at $\pm 2.5\ \mu\text{eV}$ and the other at $\pm 4\ \mu\text{eV}$. Tunneling spectra measured with partially filled pores display peaks at $\pm 4.0\ \mu\text{eV}$ corresponding to tunneling of molecules near the pore walls and show that the peaks at $\pm 2.5\ \mu\text{eV}$ in the filled pores, which are similar to bulk solid peaks, can be attributed to molecules in the center of the pore. The lowest-lying librational excitation of the methyl group exhibits behavior consistent with a two-component system with a bulk solidlike librational excitation and a lower-energy librational peak due to the surface molecules. The methyl dynamics are well-described as one-dimensional rotationally hindered rotors, with the core molecules under the influence of a single hindering barrier while the surface molecules experience a distribution of barrier heights. Quantitative estimates of this distribution are presented. Finally, the temperature dependence of the tunneling spectra for both the completely filled and partially filled pores is discussed.

DOI: 10.1103/PhysRevB.63.014301

PACS number(s): 66.30.-h, 78.70.Nx, 29.30.Hs, 33.20.Sn

I. INTRODUCTION

Quantum rotational tunneling is extremely sensitive to both the shape and magnitude of intermolecular potentials.¹⁻⁵ Thus the experimental determination of tunneling spectra using techniques such as nuclear magnetic resonance or neutron scattering can provide detailed information on intermolecular potentials. Due to the large incoherent neutron-scattering cross section present in the (usually) hydrogenous tunneling species, rotational tunneling can often be observed using high-resolution neutron scattering. When scattering from hydrogenous systems, the interpretation of the data is straightforward due to the single-particle nature of the interaction between the neutron and sample.¹ Therefore neutron scattering is an ideal choice for investigations of rotational tunneling.

Tunneling in various restricted geometries has been studied for several systems, but especially for methane (see compilation by Prager and Heidemann⁴ for a recent list of confined methane studies). Methane has a rich tunneling spectrum in the bulk solid phases. When confined to various porous glasses, the tunneling rotors behave as though they are under the influence of a distribution of orientational potentials as opposed to the much simpler potential in the bulk solid phase.^{6,7} The extensive studies of solid mixtures of methane and krypton provide an excellent demonstration of the use of tunneling as a probe of local orientational disorder.⁸⁻¹⁰

Methyl iodide (CH_3I) is a textbook example of a one-dimensional quantum rigid rotor.¹¹ In the bulk solid phase at low temperatures ($T < 40\text{ K}$) the methyl rotors experience a threefold symmetric potential that hinders the reorientation of the molecule about the I - C axis. This single-particle potential can be expressed as $V(\phi) = V_3[1 - \cos(3\phi)]/2$, where ϕ is the angular coordinate characterizing the orientation of the methyl rotor about the I - C axis. If the rotational barrier

V_3 is not too large the hydrogen wave functions will overlap appreciably. Then, if the thermal energy is well below that of the potential barrier, the hydrogen atoms can tunnel through the potential barrier. In a neutron-scattering measurement the tunneling frequency manifests itself as a discrete energy transfer to (or from) a neutron. Tunneling energies typically are small (≤ 1 to a few $100\ \mu\text{eV}$) and necessarily require high-resolution neutron measurement techniques such as backscattering. Neutron backscattering spectra of bulk methyl iodide at 5 K show well-defined tunneling peaks at $\pm 2.4\ \mu\text{eV}$ (0.6 GHz).¹¹ As the temperature is raised to about 20 K these peaks move to slightly higher energies due to a distortion of the single-particle potential from phonons. Subsequent temperature increase causes the tunnel peaks to move inwards (due to increased thermal population of the rotational levels) towards the elastic line until, at 40 K , the scattering appears quasielastic, indicative of classical hopping of the methyl groups over the potential barrier. Thus there is a continuous transition from the quantum tunneling regime to classical rotational hopping. In light of these results, CH_3I confined in a nanoporous medium provides an ideal probe of local disorder, surface interactions, and the effects of confinement.

To our knowledge the only previous neutron-scattering study of confined methyl iodide was performed for CH_3I on graphite.^{12,13} For this case, neutron diffraction demonstrated that the molecule's threefold molecular axis lies parallel to the surface. Tunneling of the methyl groups was observed at $40\ \mu\text{eV}$ for momentum-transfer parallel to the graphite surface and $20\ \mu\text{eV}$ for polarizations parallel and perpendicular to the surface. Thus the presence of the surface significantly decreases the rotational potential. More recently Loughnane and Fourkas have used optical Kerr-effect (OKE) spectroscopy to study the relaxation response of CH_3I in porous silica gels ($d_{\text{pore}} = 24\text{--}83\ \text{Å}$).¹⁴ At temperatures between 200 and 320 K , two distinct relaxation rates were measured

which were subsequently assigned to bulklike CH_3I and CH_3I molecules strongly influenced by the presence of the surface. Raman measurements of confined methyl iodide in silica glasses with pore sizes ranging from 12 to 70 Å indicate that methyl iodide confined to smaller pores has a higher degree of orientational order and a slower relaxation rate than that confined in larger pores.¹⁵

Here we present the results of a series of inelastic incoherent neutron-scattering measurements performed on the molecular system methyl iodide confined to porous glass monoliths with a narrow pore size distribution centered around 58 Å. The remainder of this paper is laid out as follows. In Sec. II we discuss details of the experimental technique including sample preparation. In Sec. III we present the results, along with fits to the neutron-scattering data. In Sec. IV we discuss the interpretation of our results. We finish with a summary and brief discussion of future measurements.

II. EXPERIMENTAL DETAILS

The methyl iodide used in this paper, obtained from Sigma company¹⁶ with a stated purity of 99.4%, was used as received with no further purification. The porous glass monoliths used were obtained from Geltech, incorporated.¹⁶ Each monolith, disk shaped, with a diameter of 6 mm and thickness of 2 mm, has a monodispersed pore distribution centered about 58 Å with a 10 Å full width at half maximum (FWHM), an open pore volume of about 63%, and a specific surface area of 534 m²/g as determined by nitrogen adsorption/desorption isotherm measurements. They were heated to 800 °C to remove impurities and kept under vacuum while being shipped to NIST. Upon receipt the disks were transferred into a vial containing liquid CH_3I , sealed, and allowed to soak for 48 h. Note that in this paper no surface treatment was performed to remove hydroxyl groups from the surface of the porous glass as was done in previous Raman and OKE measurements.^{14,15} Previous investigations into adsorption of CH_3I onto silica gels provide compelling evidence that the methyl iodide molecules preferentially adsorb onto surface sites with free OH groups. Therefore surface treatment will likely affect the surface-molecule interaction and hence the areal density of adsorbed molecules.¹⁷

Gravimetric measurements of the disks saturated with the liquid at room temperature indicate an approximately exponential desorption with a time constant of about 5 min. After soaking in the liquid for 2 days, 11 disks were transferred to a cylindrical aluminum sample cell wide enough to provide a snug fit for the disks. Upon completion of the measurement, the disks were weighed as soon as the cell was opened and the mass corresponded to a pore filling of $95 \pm 5\%$. We will refer to the 95% filled pores as “full pores.” Measurements were also performed using disks that were partially filled with CH_3I . This was achieved by allowing the disks to desorb for a fixed period of time before transferring them to the cell and sealing it. Upon completion of the measurement the disks were again weighed as soon as the cell was opened. The mass indicated that the disks were approximately $55 \pm 7\%$ filled with CH_3I . We will henceforth refer to these as

the “partially filled pore” samples.

All neutron-scattering measurements were carried out at the NIST Center for Neutron Research. The tunneling measurements were performed on the new NIST high-flux backscattering spectrometer (HFBS).¹⁸ HFBS is a high-energy resolution backscattering spectrometer in which the incident neutron energy is varied via Doppler shifting the neutrons about a nominal incident wavelength of 6.271 Å. After scattering from the sample only neutrons with a fixed final energy are received in the detectors as determined by Bragg reflection from a large crystal analyzer system. In all spectra the data were summed over 9 detectors spanning momentum transfers between 0.62 to 1.5 Å⁻¹ and normalized to the total incident beam monitor counts. The instrument was operated with a dynamic range of $\pm 27 \mu\text{eV}$ (energy transfer) with an energy resolution of 1 μeV .

The measurements of the librational excitations were performed using the new filter analyzer neutron spectrometer (FANS). The incident neutron energy is monochromated via the 002 reflection from a pyrolytic graphite monochromator. After scattering from the sample only neutrons with final energies less than 1.8 meV are counted in the 48 detectors spanning scattering angles between 17.9° and 118.3°. This is accomplished using a composite analyzer made up of a combination of polycrystalline beryllium, followed by a block of polycrystalline graphite, which determines the effective analyzer energy resolution, which in this case is about 1.1 meV. All spectra presented here are the result of summing over all detectors and normalizing to the incident beam monitor.

In all measurements the sample cell was mounted onto a sample probe in a top-loading helium flow cryostat. The temperature of the sample cell was determined via silicon diode thermometer. The measurements performed on HFBS were done at temperatures between 5 K and 40 K while the measurements done on FANS were performed at 5 K only. Reference measurements of the bulk molecular solid were performed on both instruments in order to provide a direct comparison between the bulk and confined systems. In both measurements on bulk CH_3I , the sample was contained in a sealed annular aluminum sample cell in order to minimize multiple scattering.

III. RESULTS

Figure 1 shows tunneling spectra for the partially filled, full-pore, and bulk cases at 5 K. There are a number of notable features in the full pore data. First, there is a large elastic-scattering component due to scattering from the sample can, the porous substrate, and a portion of the molecular solid structure. A measurement of the empty Geltech disks at 5 K revealed nothing more than elastic scattering and a flat background, so no attempt to subtract the background was performed. The inelastic spectra contain two sets of tunneling peaks on the Stokes and anti-Stokes sides of the elastic line. It is clear from the figure that the two smaller peaks near $\pm 2.5 \mu\text{eV}$ for the confined solid, which are resolution limited, are comparable in position and shape to the bulk tunneling peaks. The other set of tunneling peaks have an intrinsic linewidth of 1.9 μeV , which is considerably

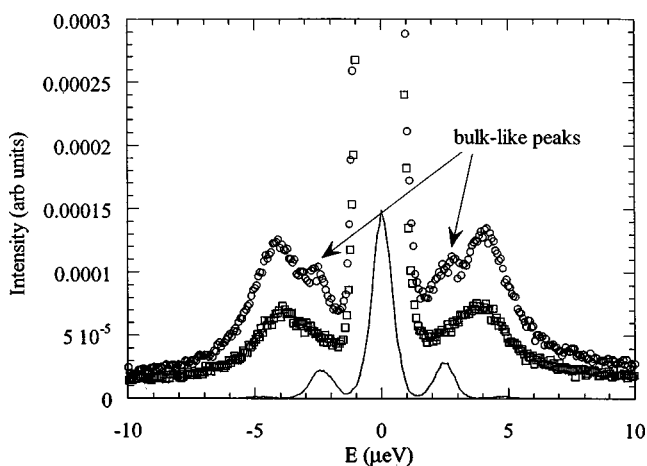
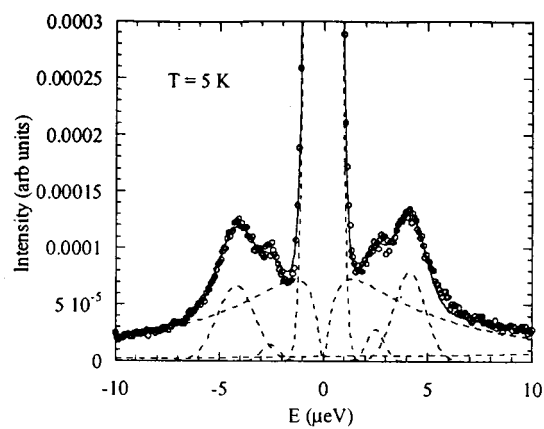


FIG. 1. Tunneling spectra collected at 5 K for the full pore sample (circles), partially filled pores (squares), and the bulk sample (solid line). Bulk data has been scaled down by a factor of 100 for clarity.

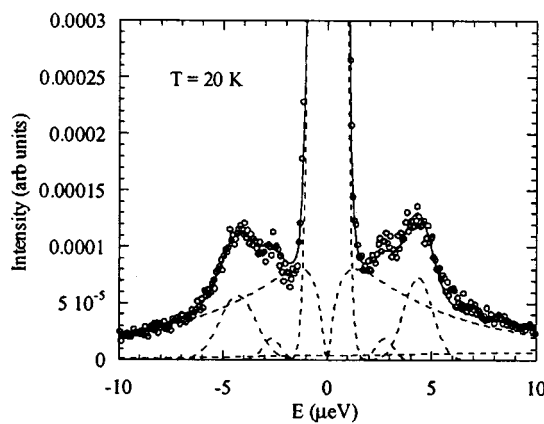
larger than the bulklike peaks and appear at higher energies, $\pm 4 \mu\text{eV}$. The spectra from the partially filled pore sample are noticeably different from the full pore case. First, the peaks near the bulklike tunnel energies have vanished leaving only a broadband peaked at higher energy. The maximum of this band is closer to the elastic line than the higher-energy peak of its full-pore counterpart.

In order to extract quantitative information from the tunneling spectra a simple model was adopted for fitting the peaks. For most of the lower-temperature full-pore spectra, we found that four Gaussians (two pairs of tunneling peaks) plus a delta function (elastic scattering), and a lognormal distribution, all convoluted with the instrumental resolution function plus a gently sloping background proved to be an excellent representation of the data. A Lorentzian line shape can replace the lognormal line shape and provide an equally good fit. However the choice of the lognormal better reflects the underlying physics, which is discussed in the next section. Representative fits are presented in Fig. 2. We will henceforth refer to the lower-energy tunneling peaks as ‘‘core’’ peaks and the higher-energy peaks as ‘‘surface’’ peaks. The central idea behind this assignment is that the lower-energy peaks arise from the bulklike solid that occupies the center, or core, of the pore, and the higher-energy peaks arise from the molecules near the pore walls. This designation is also useful when describing the partially filled pore spectra. We must also consider the possibility that the bulklike peaks are due to the presence of bulk solid located outside of the porous glass samples, perhaps on the inside walls of the sample container. However, this is unlikely since the bulklike peaks are shifted higher by 5% when compared to the tunneling energy in pure bulk CH_3I . Such shifts can be associated with a somewhat different orientational potential for molecules localized near the center of the pores.

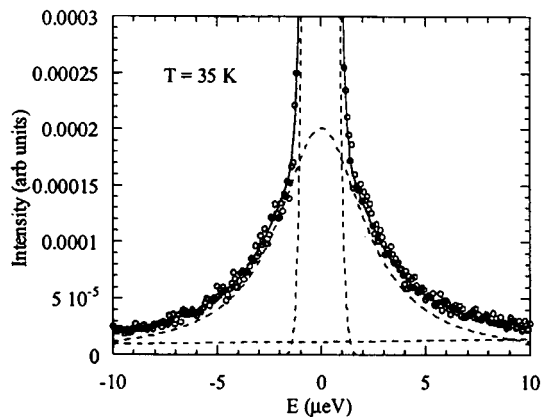
As the temperature increases, a number of changes occur in the spectrum. When the temperature is increased to 30 K it becomes impossible to distinguish between the core and surface contributions to the scattering because the two sets of tunneling peaks merge into a single pair of broad peaks. At



(a)



(b)



(c)

FIG. 2. Fits of model, as discussed in the text, to the tunneling spectra for for full-pore samples for (a) 5 K, (b) 20 K, and (c) 35 K.

35 K the tunneling peaks coalesce to form a single quasielastic-like peak and no further tunneling features are observed above 35 K. As temperature increases the width and the integrated intensity of the lognormal component remain ap-

proximately constant up to 30 K. Above 30 K a pure Lorentzian component is used to model the quasielastic scattering and the lognormal is no longer used in the fitting.

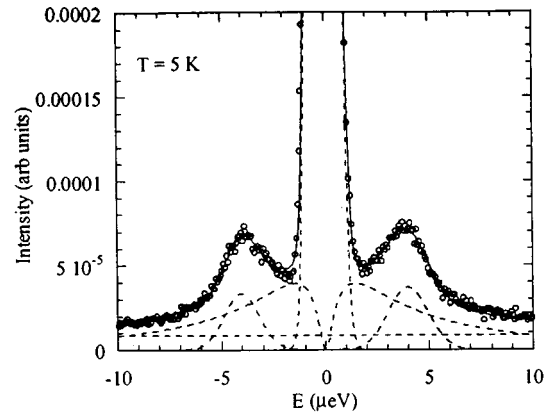
When the porous glass is partially impregnated with CH_3I , as in Fig. 3, the two bulklike peaks vanish leaving only the broad peaks at higher energy. In this set of data we fit nearly the same model as in the full-pore case except that now we only fit a single pair of Gaussians to the tunneling peaks. In addition, a broad scattering component is present even at the lowest temperature of 5 K, which again has been fit with a lognormal distribution. This broad scattering component, whose integrated intensity scales with the amount of solid present in the porous glass, is present even when the pores are partially filled with the solid. Thus we believe that this feature is associated with the first few adsorbed layers of the CH_3I . This model provides an excellent fit to the data presented in Fig. 3. Once again the peaks merge and coalesce into a single quasielastic peak as the temperature approaches 35 K.

The temperature dependencies of the peak positions for both the core and surface components are shown in Fig. 4. The tunneling peak positions of the bulk solid are plotted for reference. In the bulk solid, the peak energies exhibit an interesting temperature dependence. There is a small increase in the peak positions up to 25 K ($0.16 \pm 0.03 \mu\text{eV}$) and then the usual softening, typical of tunneling systems.^{1,4} Although higher in energy, the temperature dependence of the “surface” tunnel peaks in the full-pore sample appear to follow a similar trend to the bulk. The temperature dependence of the core peak positions are consistent with the bulk temperature dependence (although slightly higher in energy) but, since one pair of tunneling peaks vanishes at 30 K, it is impossible to provide a more quantitative estimate of the temperature dependence of the core peaks. For the partially filled samples, the tunneling energy for the surface component follows a similar temperature dependence as the bulk but the values at each temperature are consistently lower than the surface peaks found in the full-pore sample.

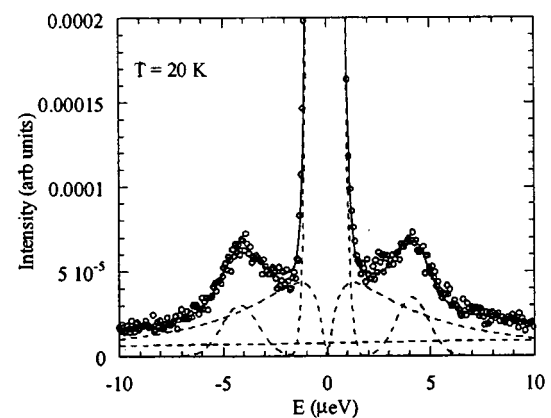
Finally we present in Fig. 5 the background corrected spectra collected on FANS, which directly reflects the density of librational states for bulk CH_3I and full-pore Geltech. The bulk data show a doublet between 12.5 and 14 meV while the confined spectra show a broad peak centered about 12 meV. Previous measurements of the bulk showed a doublet with the lower-energy portion centered about 13.27 meV.¹¹ Differences in energy calibration in the two instruments (FANS at NIST and SV-22 at KFA in Julich) could account for the differences in the location of the doublet. Previous INS measurements determined that the lower-energy component of the doublet is due to rotation about the I - C axis while the higher-energy component is due to rotation about an axis perpendicular to the I - C axis.¹¹

IV. DISCUSSION

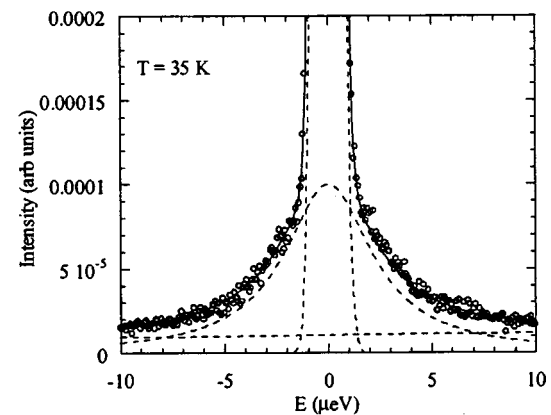
The results described in the previous section suggest a simple physical picture where two components provide dominant contributions to the inelastic spectra: (1) “surface” molecules, that is molecules that are in the first few



(a)



(b)



(c)

FIG. 3. Fits of model, as discussed in the text, to the tunneling spectra for partially filled samples for (a) 5 K, (b) 20 K, and (c) 35 K.

layers adsorbed onto the pore wall, and (2) “core” molecules, or molecules that reside near the center of the pores. Clearly this is an oversimplification since there can be no clear delineation between molecular layers. However our as-

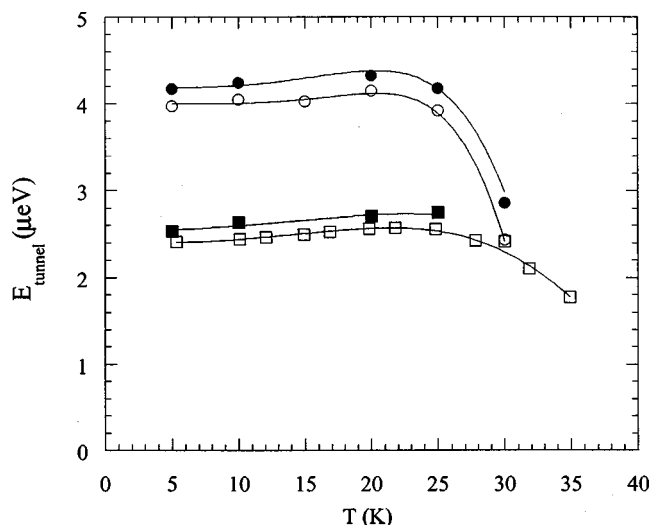


FIG. 4. Temperature dependence of the peak position of the surface (open circles) tunneling peaks for the partially filled samples, surface peaks for the full pores (solid circles), and core peaks (solid squares). The temperature dependence of the bulk tunneling lines are presented for reference (open squares). Solid lines are fits to a theoretical model as described in the text.

signment of distinct populations of surface and core molecules is consistent with the interpretation of the OKE measurements on liquid CH_3I .¹⁴ Moreover the comparison of the full-pore case with two sets of two tunneling peaks and the partially filled pore case where the bulklike peaks vanish, but the higher-energy peaks remain, also supports this simple picture.

In bulk CH_3I , one can use the location of the tunneling peaks at low temperature to determine the potential barrier, which hinders rotation. Since the system is, to a very good approximation, a one-dimensional quantum rotor, the Schrodinger equation can be solved numerically, and one can extract the corresponding tunneling energies as a function of barrier height. The Hamiltonian can then be expressed as

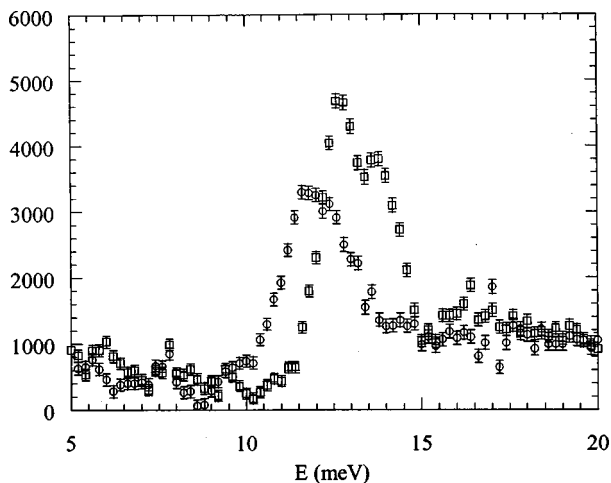


FIG. 5. Density of librational states for bulk (squares) and confined (circles) CH_3I .

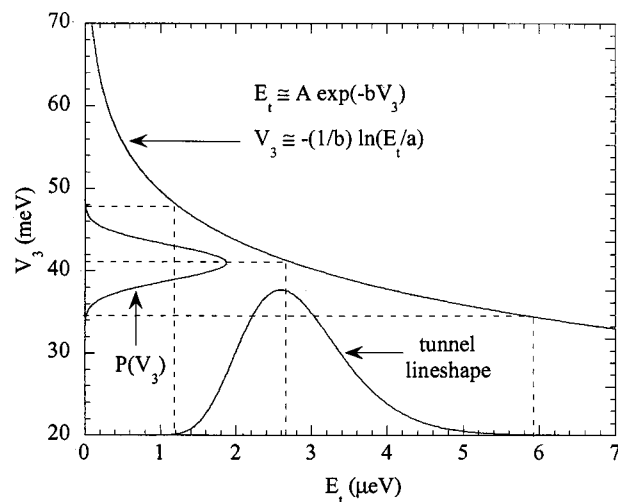


FIG. 6. Graphical illustration of the effects of a distribution of potential barriers on the tunneling line shape. Asymmetry of line is due to nonlinear (exponential) dependence of tunneling energy on the barrier height. Parameters A and b are found from a fit to results of the numerical solution of Eq. (1).

$$H = -\frac{\hbar^2}{2I} \frac{\partial^2}{\partial \phi^2} + \frac{V_3}{2} (1 - \cos 3\phi), \quad (1)$$

where I is the moment of inertia of CH_3 , the methyl rotor, V_3 is the barrier height, and ϕ is the angular coordinate of the rotor. The resulting eigenvalues of the Hamiltonian (1) can be calculated as a function of V_3 .¹⁴ The tunneling energy, defined as the splitting between the $J=0$ and $J=1$ rotational states of the free rotor,¹⁹ has an approximate exponential dependence on the barrier height V_3 . Using this dependence on barrier height, and the fact that the bulk tunnel peaks measured at 5 K on HFBS occur at $\pm 2.4 \mu\text{eV}$, we find that the $V_3 = 42.0 \pm 0.2 \text{ meV}$, in good agreement with the values obtained previously using nuclear-magnetic resonance (NMR) (41.8 meV) and neutron scattering (41 meV).⁴ Previous measurements⁴ suggest a small sixfold contribution to the hindering potential, but its effects are small and we have decided to ignore this term for simplicity.

It is clear from Figs. 2 and 3 that the tunneling peaks due to the surface molecules have an intrinsic width. This width could be due to an increased population of the excited states resulting in a thermally activated linewidth of the form $\Gamma = \Gamma_0 e^{-E/kT}$ as is found in the bulk.¹¹ Since there is relatively little temperature dependence to the peak widths within the resolution of the spectrometer, we can rule out this possibility. Alternately, the width could be due to a distribution of hindering potential barrier heights V_3 . In this case, we can extract the distribution directly from the tunneling line shape. We simply use the relationship between the tunneling energy and the potential barrier height found from the numerical calculations of Eq. (1) and perform the transformation from the resolution corrected tunneling line shape to potential barrier as shown in Fig. 6. Before doing so however, we must consider the underlying broad scattering component observed in all of the low-temperature tunneling spectra.

In each of the sets of low-temperature tunneling spectra the very broad scattering component, which underlies the well-defined tunnel peaks, can be attributed to disordered methyl rotors and provides the motivation for using the log-normal distribution in the fit. In a tunneling system where the tunnel energy has an exponential dependence on barrier height, a Gaussian distribution of barrier heights yields a lognormal line shape. This type of broad scattering has been observed in other systems possessing methyl groups and there is ample evidence that this component is a disorder effect.^{8,20–23} Recent neutron backscattering spectra for the polymer system poly(vinyl-acetate) where the scattering is predominantly from methyl groups, display a broad temperature-independent scattering component at temperatures as low as 2.4 K.²⁰ At such low temperatures it is highly unlikely that this scattering arises from the diffusive motion of the molecules, because the activation energy for such a diffusive process would have to be on the order of 2.4 K or about 210 μeV , characteristic of an almost free rotor. The interpretation presented by Colmenero and co-workers²⁰ is that the methyl groups in the disordered polymer environment see a very broad distribution of hindering potentials and, in fact, it is quantum rotational tunneling of the methyl rotors that provides the apparent “quasielastic” scattering component.

Similarly, a broad scattering component is observed in the confined CH_3I spectra down to 5 K. Completely analogous arguments lead us to conclude that this intensity must be due to tunneling of methyl groups in a highly disordered environment. Since it is present even in the partially filled sample spectra, this feature must be associated with the molecules adsorbed onto or near the pore wall. Up to now we have assigned the resolution-limited peaks near $\pm 2.5 \mu\text{eV}$ to the core region and the peaks at $\pm 4 \mu\text{eV}$ to the molecules near the surface. Perhaps a better designation is in terms of the degree of order of the local environment and its effects on the intermolecular potential felt by the methyl groups. Thus in the full-pore samples, we expect that the core molecules experience a locally highly ordered environment resulting in resolution-limited tunneling peaks (as in the bulk ordered system). The surface molecules, however, must be subdivided into two further classifications: those with small degree of disorder in their local environment and those with a large degree of disorder. Those surface molecules with a small degree of disorder in their environment appear as the inelastic peaks seen at $\pm 4 \mu\text{eV}$ with some intrinsic width and those with more disorder appear as the broad scattering. From this characterization a qualitative picture of the structure emerges. In the center of the pore we have the ordered solid, very similar in structure to the bulk solid. As we move away from the center of the pore towards the pore wall, the molecules begin to deviate from the bulklike structure until, at the pore wall, they are in a highly disordered state, perhaps in an attempt to arrange themselves with the disordered surface of the wall.

We can estimate the amount of disorder necessary to cause each of the scattering components by considering a distribution of hindering potentials for each one. Using the full-pore data at 5 K, we can fit barrier-broadened tunneling

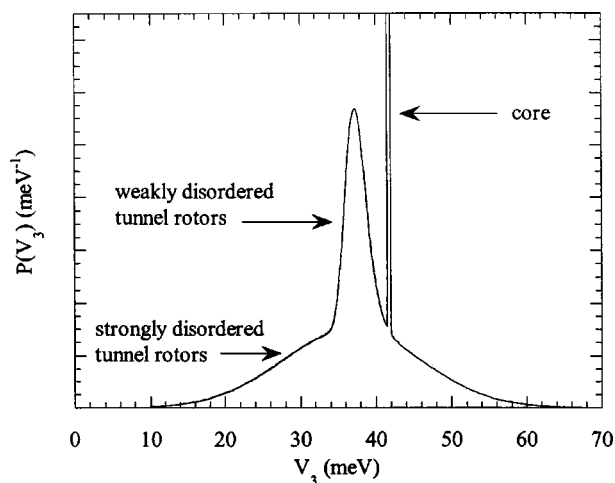


FIG. 7. The total barrier height probability distribution extracted from the full-pore spectra reflecting the highly ordered core rotors, weakly disordered surface rotors, and the strongly disordered surface rotors. Relative contributions have been scaled to the integrated intensity of each component in the tunneling spectra.

line shapes (Fig. 6) to the broad scattering component and the surface peaks and resolution limited lines to the core peaks. As can be seen in Figs. 2 and 3, this provides an excellent description of this component of the scattering. The distribution of barrier heights that we extract from such a fit is shown in Fig. 7. The center of the distribution for the strongly disordered component occurs at 36.8 meV with a FWHM of about 22.5 meV. The center of the barrier distribution coincides roughly with that of the surface molecules (38 meV), which provides even more evidence that this scattering feature is associated with molecules on or near the pore wall. The uncertainty in the probability density, $P(V_3)$, extracted from the tunneling measurements, is difficult to quantify for the broadest component at very high values of V_3 ($>55 \text{ meV}$) and very low values of V_3 ($<25 \text{ meV}$). This limitation is due to the finite dynamic range of the spectrometer for low barrier heights and the finite instrumental resolution for larger barrier heights. Thus the tunneling measurements provide the most reliable information on the probability density encompassed in the region near the core and weakly disordered tunnel rotors.

Using the integrated intensities found in the tunnel spectra we can also make a rough estimate of the amount of CH_3I in each of the three environments. Based on the fits to the 5 K tunnel spectra for the full-pore case, about 70% of the scattering intensity arises from strongly disordered surface rotors, $\sim 25\%$ comes from the weakly disordered surface rotors, and only $\sim 5\%$ comes from the core rotors. If we further assume that the pores are perfectly cylindrical with no dispersion in the pore-size distribution and that the density of the confined solid is the same as the bulk liquid, then we estimate that the strongly disordered surface rotors are constrained to three solid layers next to the pore walls, the weakly disordered surface rotors make up the next two layers, and the “ordered” rotors fill the remaining central region of the pore. The assumption of perfectly monodispersed pore sizes is incorrect since we know that the pore size dis-

tribution has a 10% breadth. Nevertheless, this model enables us to predict that confinement in larger pores would result in a larger core contribution while confinement in smaller pores would eliminate this contribution completely. Measurements are planned to test this hypothesis.

The small energy shifts of the surface tunneling peaks in the full-pore system compared to the partially filled pore case provide insight as to the effects of the surface of the porous glass and the presence of the core molecules. The distribution of potentials for the surface molecules in the full-pore case and partially filled case have the same width but the full-pore distribution is located at a slightly lower-potential energy (37.8 meV) than the partially filled case (38.0 meV). This suggests that the presence of the core molecules tends to reduce the potential experienced by the surface molecules presumably due to small structural changes. For the full-pore sample the core barrier distribution is located at an energy that is lower than the bulk by about 0.35 meV, less than a 1% shift. This indicates that the presence of the glass surface (and perhaps the surface molecules themselves) tends to reduce the potential barrier experienced by the core molecules when compared to a CH_3I molecule in the bulk solid.

The spectrum for the low-lying librational modes can also be estimated using Eq. (1) and the picture of the potential barriers presented above, and the result can be compared with the measurements taken on FANS (Fig. 5). There are two contributions to the tunneling spectrum in the full-pore sample so we can assume the same for the librational excitations. Based on the numerical calculations of Eq. (1) and the tunneling data, the bulklike methyl groups in the core experience a potential barrier of 42 meV while the surface molecules feel a potential barrier of 37.8 meV. These barriers predict librational modes of 14.00 meV and 13.17 meV, respectively, differing by 0.83 meV.

The first librational mode in the bulk spectra shown in Fig. 5 occurs at an energy transfer of 12.63 ± 0.04 meV, based on a two-Gaussian fit to the doublet. In order to estimate the contribution to the librational spectrum from CH_3I molecules near the pore wall, we can subtract an appropriate fraction of the bulk FANS spectra from the confined FANS spectra. The bulklike portion subtracts out quite well leaving a well-defined peak at 11.81 ± 0.02 meV, which we attribute to the molecules near the pore wall (Fig. 8). The difference in energy between the bulk librational mode and the surface librational peak is 0.82 ± 0.04 meV, which is in excellent agreement with the numerical estimate of 0.83 meV based on our tunneling measurements. So while the absolute value of the librational energy is slightly overestimated by the model, the energy difference is in complete agreement with that based on the tunneling data.

The intrinsic width of this librational peak (after correcting for instrumental resolution) is 1.1 ± 0.1 meV. We can attempt to relate this width to the distribution of barrier heights as we did for the widths of the tunneling peaks via numerical calculations of the librational energies over a range of barrier heights. The resulting distribution has a width of 2.24 meV (inset of figure) which is larger than the width of the distribution obtained from the breadth of the tunneling lines (1.47 meV). One possible explanation for the larger distribution

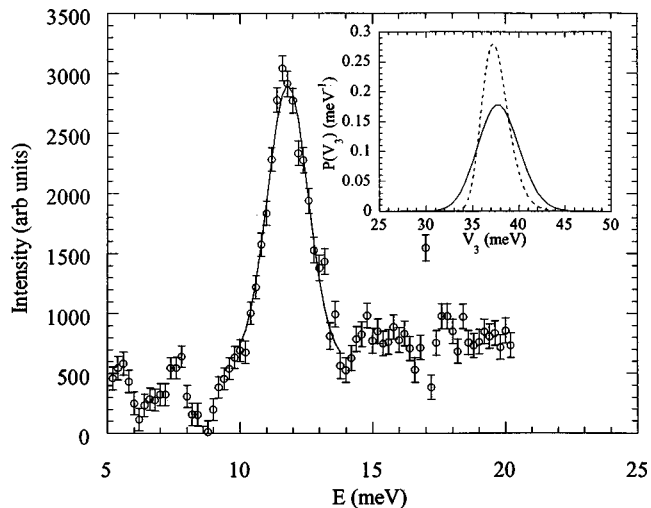


FIG. 8. Density of librational states for the surface molecules extracted from the full-pore samples and a subtraction of the bulk density-of-states as described in the text. Inset: the distribution of barrier heights extracted from the librational density-of-states for the surface molecules (solid line) and the distribution extracted from the tunnel spectra (dashed line).

from the FANS data compared with the HFBS data is that there could be an unresolved line in the spectrum shown in Fig. 8. The doublet observed in the bulk spectrum is composed of two peaks, due to librations about different axes. It is entirely possible, in fact likely, that an unresolved line exists in the surface librational spectrum, which would lead to an apparent broadening of the observed librational line. Another possible explanation for the larger width is that there is a broad contribution to the spectrum near this excitation energy due to a disordered array of molecules near the pore wall.

It would be interesting to know how the molecules are arranged within the pores, since an understanding of this structure could lead to further understanding of the origin of the distribution of potential barriers. It is expected that the dynamics of surface molecules, which have the C_3 axis perpendicular to the pore wall, will be substantially different than those whose threefold axis is parallel to the pore wall.²⁴ In the case of a polar molecule like CH_3I in porous silica, the electric fields set up by the hydroxyl groups on the silica surfaces should force the surface molecules to align their I-C axes perpendicular to the pore wall.¹⁷ Unfortunately our current measurements can make no distinction between these two cases but we expect that there will be differences in the forces felt by the surface molecules and the core molecules.

The temperature dependence of the tunneling lines provides clues as to how the methyl groups interact with the phonons in the solid. One possible effect of confinement is that the temperature dependence of the tunneling lines will be influenced by the density-of-states of the phonons in the porous substrate. Prager *et al.* have presented an empirical expression that characterizes the unusual temperature dependence of the tunneling lines in bulk CH_3I .¹¹ This expression is written as

$$\frac{E_t(T)}{E_t(0)} = \frac{1 - \exp(-E_c/k_B T)}{1 - (1 + A_c)\exp(-E_c/k_B T)} - A_s \exp(-E_s/k_B T), \quad (2)$$

where $E_t(T)$ is the tunneling energy at temperature T , E_c is the phonon energy in the Einstein approximation, E_s is related to the librational energy, and A_c is related to the coupling of the phonons to the methyl rotors.¹¹

In order to provide a quantitative comparison of the temperature dependence we have fit each of the sets of tunneling peaks to this model as shown in Fig. 4 but held the librational energy E_s , fixed to its value derived from the tunneling spectra. We find that the phonon energy depends strongly on which scattering component is examined. For the bulk CH_3I we find that the phonon energy $E_c = 2.94$ meV, in rough agreement with Prager *et al.*¹¹ who found that $E_c = 2.15$ meV. The fit to the temperature dependence of the core molecules yields a phonon energy of 1.78 meV and to that of the surface molecules, 5.39 meV. It is not clear whether we can relate these energy shifts to a change in the phonon density-of-states due to the presence of the porous substrate or if it is a density effect. The lack of any detailed structural information precludes us from making any conclusive statements regarding the origin of these energy shifts.

V. SUMMARY

This paper demonstrates that we can apply the same model of one-dimensional hindered rotation to the confined CH_3I system as we can in the bulk solid, albeit with a number of different CH_3I environments in the confined system. The tunneling of CH_3I is an ideal probe of the local environment in confined geometries. The high-resolution neutron-scattering measurements, presented here, of CH_3I confined to porous glass monoliths, reveal a substantial modification of the tunneling spectrum when compared with the bulk spectrum. When the porous glass is fully impregnated with the solid, two distinct pairs of tunneling peaks are observed. One

set occurs at about ± 2.5 μeV and the other at ± 4 μeV . Pores that are partially filled with the solid exhibit only the peaks near ± 4 μeV . We attribute the peaks at ± 2.5 μeV in the full-pore case to molecules located near the center of the pore, which have a very high degree of local order, similar to those in the bulk solid. The broad peaks located at ± 4 μeV in both cases are due to molecules located at or near the pore wall. The breadth of these peaks arises from a local distribution of orientational potentials. The tunneling peaks associated with the molecules near the pore wall are consistent with our measurement of the librational density-of-states for the confined solid. A temperature-independent broad scattering feature is found in both the full-pore and partially filled pore tunneling spectra that we associate with disordered methyl rotors. We have quantified the local disorder in the confined solid using the one-dimensional model and the neutron-scattering spectra to obtain a probability distribution of orientational potentials for each of the CH_3I components. Further measurements are planned of the tunneling of CH_3I confined to glasses with smaller pore sizes as well as with and without surface treatment in order to further characterize the effects of surface interactions.

ACKNOWLEDGMENTS

We are grateful to Dennis Minor of the NIST Ceramics Division for performing the adsorption/desorption measurements of the silica samples, Peter Papanek, Nick Maliszewskij, Donald Pierce for their assistance with the new filter analyzer neutron spectrometer at NIST, Dan Dender and Louis Santodonato for assistance with the cryogenics, Rob Myers at Geltech, Inc., Sam Trevino of the U.S. Army Research Laboratory, Christopher Soles of the NIST Polymers Division, and Paul Sokol at Pennsylvania State University for useful discussions. Finally we are grateful to John J. Rush and Andreas Meyer for a critical reading of the manuscript.

*Corresponding author

¹W. Press, *Single-Particle Rotations in Molecular Crystals* (Springer-Verlag, Berlin, 1981).

²A. J. Horsewill, *Spectrochim. Acta, Part A* **48**, 379 (1992).

³C. J. Carlile and M. Prager, *Int. J. Mod. Phys. B* **7**, 3113 (1993).

⁴M. Prager and A. Heidemann, *Chem. Rev.* **97**, 2933 (1997).

⁵R. K. Thomas, *Prog. Solid State Chem.* **14**, 1 (1982).

⁶D. Balszunat, B. Asmussen, and M. Muller *et al.*, *Physica B* **226**, 185 (1996).

⁷C. Gutt, B. Asmussen, I. Krasnov, W. Press, W. Langel, and R. Kahn, *Phys. Rev. B* **59**, 8607 (1999).

⁸S. Grondey, M. Prager, W. Press, and A. Heidemann, *J. Chem. Phys.* **85**, 2204 (1986).

⁹S. Grondey, M. Prager, and W. Press, *J. Chem. Phys.* **86**, 6465 (1987).

¹⁰B. Asmussen, W. Press, M. Prager, and H. Blank, *J. Chem. Phys.* **98**, 158 (1993).

¹¹M. Prager, J. Stanislawski, and W. Hausler, *J. Chem. Phys.* **86**, 2563 (1987).

¹²R. E. Bucknall, S. M. Clarke, R. A. Shapton, and R. K. Thomas, *Mol. Phys.* **67**, 439 (1989).

¹³S. M. Clarke and R. K. Thomas, in *Dynamics of Molecular Crystals*, edited by J. Lascombe (Elsevier, Amsterdam, 1987), pp. 365–376.

¹⁴B. J. Loughnane and J. T. Fourkas, *J. Phys. Chem. B* **102**, 10 288 (1998).

¹⁵Y. T. Lee, S. L. Wallen, and J. Jonas, *J. Phys. Chem.* **96**, 7161 (1992).

¹⁶Manufacturers are identified in order to provide complete identification of experimental conditions, and such identification is not intended as a recommendation or endorsement by NIST.

¹⁷T. Ishikawa, E. Amano, M. Muroya, and S. Kondo, *Chem. Lett.* **4**, 415 (1983).

¹⁸P. M. Gehring and D. A. Neumann, *Physica B* **241-243**, 64 (1998).

¹⁹In the limit that $V_3 \rightarrow 0$, the eigenvalues are those of a free methyl rotor with $E = BJ^2$ ($B = 0.65$ meV) whereas for a large barrier height the eigenvalues approach those of a torsional oscillator.

Note that J is only a good quantum number for this system in the limit that $V_3 \rightarrow 0$.

- ²⁰J. Colmenero, R. Mukhopadhyay, A. Alegria, and B. Frick, Phys. Rev. Lett. **80**, 2350 (1998).
- ²¹A. J. Moreno, A. Alegria, J. Colmenero, and B. Frick, Phys. Rev. B **59**, 5983 (1999).
- ²²J. Colmenero, A. J. Moreno, A. Alegria, R. Alvarez, R. Mukhopadhyay, and B. Frick, Physica B **276-278**, 322 (2000).
- ²³A. J. Moreno, A. Alegria, J. Colmenero, and B. Frick, Physica B **276-278**, 361 (2000).
- ²⁴J.-P. Korb, S. Xu, F. Cros, L. Malier, and J. Jonas, J. Chem. Phys. **107**, 4044 (1997).